EXPERIMENTAL ELASTIC STRESS ANALYSES OF CYLINDER-TO-CYLINDER SHELL MODELS AND COMPARISONS WITH THEORETICAL PREDICTIONS*

J.M. CORUM, W.L. GREENSTREET,

Applied Mechanics Section, Reactor Division,
Oak Ridge National Laboratory, Oak Ridge, Tennessee, U.S.A.

ABSTRACT

Two carefully machined cylinder-to-cylinder shell models were tested, and the experimentally determined stresses were compared with theoretical predictions obtained from a thin-shell finite element analysis. The models were idealized structures consisting of two circular cylindrical shells intersecting at right angles. The first model tested had a nozzle-to-cylinder diameter ratio of 0.5 and a diameter-to-thickness ratio of 100 for both nozzle and cylinder. The second model had a nozzle-to-cylinder diameter ratio of 0.129. The diameter-to-thickness ratio was 50 for the cylinder and 7.68 for the nozzle. Both models were strain gaged and subjected to 13 separate loading cases. Comparisons of measured and predicted stress distributions are presented for three of these loadings – internal pressure and in-plane and out-of-plane moments applied to the nozzles. The analytical predictions were obtained using a finite element program that used flat-plate elements and which considered five degrees of freedom per node in the final assembled equations. The agreement between these particular finite element predictions and the experimental results is shown to be reasonably good for both models.

1. INTRODUCTION

Intersecting cylindrical shell configurations are common in structural components for nuclear reactor systems. Piping tees and nozzles in cylindrical vessels are specific examples. Despite their common occurrence, however, proven elastic stress analysis methods have not been generally available, and consequently accurate design information for such configurations has also been generally lacking. This is true even for idealized configurations consisting of two cylindrical shells intersecting normally, with no transitions, reinforcements, or fillets in the junction region.

To meet the need for experimental data obtained from carefully machined models, the U.S. Atomic Energy Commission's Oak Ridge National Laboratory is testing a series of four thin-shell cylinder-to-cylinder models as depicted in Fig. 1. In addition to serving a basic need for test results for use in developing and evaluating potential analytical techniques, the models in the series will provide design information applicable to nozzles in cylindrical

*Research sponsored by the U.S. Atomic Energy Commission under contract with the Union Carbide Corporation.

vessels and to a class of thin piping tees as well. The results will be particularly applicable to the relatively thin-walled structures of liquid-metal, fast-breeder reactor components.

Models 1 and 3 in Fig. 1 have been tested, and the experimentally determined stress distributions were compared with the predictions of a thin-shell finite element analysis. This paper describes the tests and analyses of these two models and presents representative comparisons of theory and experiment for three typical loadings – internal pressure and out-of-plane and in-plane bending moments applied to the nozzles.

The first model, which is the one pictured in Fig. 1, had a cylinder outside diameter of 10.0 in. and a nozzle outside diameter of 5.0 in. The outside diameter-to-thickness ratio of both shells was 100, which is well within the usual bounds of thin-shell theory. Model 3 also had a cylinder outside diameter of 10.0 in., but the nozzle outside diameter was only 1.29 in. The outside diameter-to-thickness ratio was 50 for the cylinder of model 3 and 7.68 for the nozzle. Thus, the nozzle thickness was such that the nozzle of model 3 was outside the usual bound of thin-shell theory.*

The first model is shown schematically in Fig. 2 together with the applied forces and moments to which it was subjected. The major dimensions are also shown. One end of the model was rigidly fixed, or "built-in," as shown, while external loads were applied to the free end of the cylinder and to the end of the nozzle. Three mutually perpendicular force components and three mutually perpendicular moment components were applied individually at each location. Thus, including internal pressure, there was a total of 13 loading cases. These 13 loading cases were each examined experimentally and analytically and the results were compared.

Model 3 was tested in the same manner as model 1; the same 13 loading cases were examined experimentally and analytically. The lengths along the cylinder and the location of the plane of load application at the free end of the cylinder, as shown in Fig. 2 for the first model, were the same for model 3. For the nozzle, however, the 19 1/2 in. and 1 1/2 in. dimensions of model 1 were 14 1/2 in. and 1 in., respectively, for model 3. The same thin-shell finite element computer program was used for both models even though it was recognized that the nozzle of model 3 could not be classed as a thin shell.

2. EXPERIMENTAL ANALYSES

Since geometrical imperfections can play a very significant role in the behavior of thin shells, extreme care was used in making the models. Both models were carbon steel. Model 1 was machined from a weldment made from two thick-walled cylinders, while model 3 was machined from a solid forging. In both cases the structure was annealed at several points during the machining process. Dimensional inspections of the finished models indicated that the geometric variations were minimal.

Both models were instrumented with electrical resistance strain gages on the inner and outer surfaces. The gage locations for the two models are depicted in Figs. 3 and 4 on developed views of the nozzles and cylinders. A total of 322 three-gage strain-gage rosettes was used on model 1, making 966 individual strain gages, while 162 rosettes, making 486 individual gages, were used on model 3. In both cases, approximately one-half of the gages were on the outer surface and one-half were on the inner surface. They were located "back-to-back" at the locations shown in the figures.

---

*A diameter-to-thickness ratio of 20 is often quoted as a lower bound for the applicability of thin-shell theory.

The gages were arranged in two opposite quadrants, as shown, along lines running from the junction of the nozzle and cylinder. On the first model there were four lines of gages in each quadrant. On the nozzle these lines were spaced at 30° intervals and ran axially along the nozzle. On the cylinder the gage lines were actually helical curves that were perpendicular to the junction line at the points where the nozzle gage lines intersected the junction line.

Model 3 was less extensively instrumented than model 1; as can be seen in Fig. 4, there were only five lines of gages on the nozzle and cylinder. On the nozzle these lines were again oriented in the axial direction.

The particular strain-gage rosette used on these models is a very compact foil rosette with the three individual gages arranged in a "Y" pattern. The individual gage length is 0.03 in. The rosettes were applied with an epoxy adhesive, with curing times and temperatures ranging from 10 hours at 250°F to 24 hours at 200°F.

Figure 5 shows model 3 in a loading frame being subjected to an in-plane moment loading on the nozzle. The right end of the cylinder was rigidly clamped to the heavy plate as shown. A split ring arrangement acting over a flange on the end of the cylinder was used for this purpose. The loading fixtures on the other end of the cylinder and on the end of the nozzle were attached in a similar manner. These heavy fixtures in effect constrained the end circles of the shell to remain plane circles.

In both models, stresses were calculated from the experimental strains by using modulus of elasticity and Poisson's ratio values of 30×10^6 psi and 0.3, respectively.

3. FINITE ELEMENT ANALYSES

The finite element program that was used for analysis of the two models was chosen as being reasonably representative of currently available and widely used finite element shell formulations. It uses flat-plate elements with five degrees of freedom per nodal point for the final assembled structure. The program was developed at the University of California, Berkeley, under the direction of Professor R. W. Clough. The original program was written for general shell analysis by C. P. Johnson [1],[2] and was later modified and adopted by O. Greste [3],[4] for treating the structural "K" joints of cylindrical shells found in offshore oil-drilling towers.

The basic element used in the program is a nonplanar quadrilateral that is built up of an assemblage of four component triangles as shown in Fig. 6. Within each component triangle, the in-plane membrane displacements u and v are assumed to vary quadratically over the plane of the triangle except that they are constrained to vary linearly along the one exterior edge. The resulting membrane element is referred to as a constrained-linear-strain triangle and it has two degrees of freedom at each of the five nodes.

The plate bending portion of the component triangle elements has three degrees of freedom at each of the three corner nodes — two rotations about axes in the plane of the element and the transverse displacement w. The displacement expansion for this element is due to Hsieh, Clough, and Tocher [5]. Full compatibility of displacements and slopes between triangular element boundaries is achieved by dividing the element into three subtriangles and assuming an independent cubic variation for w within each subtriangle. One of the ten terms of the general cubic is omitted in each subtriangle so that in the final assembled component triangle the normal slope varies linearly along each exterior edge. It is this feature that

insures slope compatibility in the resulting element system for plate bending problems. The 27 constants in the three cubic expressions for w within the triangular element are reduced to nine (and related to the nine nodal degrees of freedom) by internal compatibility considerations.

The total stiffness (membrane plus bending) of the triangular elements which form the components of the quadrilateral is obtained by superposition of the plate bending element and the membrane element. The membrane plus bending stresses vary piecewise linearly over the surface of the resulting triangular element.

The stiffness formulation for the quadrilateral element, as well as for the membrane and plate bending triangles, is summarized by Greste [3]. The quadrilateral element has five degrees of freedom at each node — three displacements and two rotations. In the final assembled structure, the five degrees of freedom per node consist of the three displacements and the two rotations about the shell tangent coordinates at each node. That small component of rotation about the shell normal that is due to bending* is, in effect, assumed equal to zero.

The finite element representations chosen for the two models are depicted in Figs. 7 and 8, which show, in each case, developed views of one-half of the nozzle, cylinder, and end plates. Only one-half of each structure was considered because of symmetry considerations. For model 1, there were 649 nodes, resulting in approximately 3000 equations to be solved for the unknown displacement parameters. To obtain approximately the same degree of mesh refinement in the junction region of model 3 as in model 1, it was necessary to use 993 nodes in the latter case, resulting in approximately 4500 equations.

The computer analysis of a single loading for model 3, using the mesh shown in Fig. 8, required slightly more than 3 minutes of CPU time on an IBM 360/91 computer. Up to six additional loadings can be treated simultaneously, provided the boundary conditions are the same. Each additional loading treated in this way required about 15 seconds of CPU time.

A problem arose in the analysis of model 3 with its slender nozzle that was not encountered in the analysis of model 1 or in similar models with relatively large nozzles. In the cases of bending moments applied to the end of the nozzle, it was found that the membrane-type axial bending stresses, which should have been constant along the nozzle, were dissipated with distance from the end of the nozzle. This dissipation was traced to the neglect of the rotational degree of freedom about normals to the nozzle surface and occurred in model 3 because of the relatively large deformations of the small slender nozzle. The problem was overcome by redefining the neglected sixth degree of freedom for these loading cases.

The difficulty is illustrated by the example problem shown in Fig. 9, in which the nozzle of model 3 was analyzed by fixing a row of nodes near the junction. The mesh shown in Fig. 8 for the nozzle was used, and the nozzle was subjected to a bending moment at the free end. The distribution of normalized bending stress in the outer wall of the nozzle is shown for three different analyses. Also shown is the predicted stress based on simple beam theory with $I = \pi a^3 h$ and $c = a$, where a is the radius of the midsurface and h is the nozzle thickness.

The middle curve in Fig. 9 was obtained with the component of bending rotation about normals to the nozzle surface neglected. These neglected rotations are small, and are in

*A component of bending rotation about the shell normal arises from the fact that the elements surrounding each node are not, in general, coplanar, thus giving rise to a small bending rotation resultant in the normal direction.

effect set equal to zero in the assembled set of equations. Overall equilibrium implicitly requires that small moments be imposed at each node to maintain zero bending rotation. These small constraints combine to counteract a portion of the applied moment and result in the decrease in membrane bending stress depicted in Fig. 9.

To illustrate that these nodal constraints depend on the deflection of the nozzle, the problem was reexamined using a reduced elastic modulus for a section near the fixed end. The nozzle deflection produced by the applied moment was thus increased and the bending moment was dissipated more rapidly as shown by the left-hand curve in Fig. 9.

The problem was overcome by redefining the neglected degree of freedom in the nozzle. Rather than setting the rotations about the normals equal to zero, the rotations about lines parallel to the nozzle axis were set equal to zero in the final assembled set of equations.* With this modification, the membrane bending moment remained constant, as shown by the right-hand curve in Fig. 9.

In conclusion, two significant points should be made. First, even though a computer program may be checked out for some geometries and conditions, there can be other cases for which it does not function properly. Thus, structural analysis programs must be thoroughly validated for the range of parameters over which they are expected to apply. Second, the problems introduced by considering only five degrees of freedom per node could be eliminated by retaining six degrees of freedom in the final assembled equations. However, for large systems, the five degrees of freedom treatment has a distinct advantage from the standpoint of economy of computer time.

4. COMPARISONS OF THEORY AND EXPERIMENT

Of the 13 loading cases analyzed for each model, three were chosen as being of particular importance and representative of the comparisons between theory and experiment. These three are internal pressure and out-of-plane and in-plane bending moment loadings on the nozzles. The values of the applied loads that were used are tabulated below for each model:

	Model 1	Model 3
Internal pressure (psi)	50	300
Out-of-plane moment on nozzle (in.-lb)	600	800
In-plane moment on nozzle (in.-lb)	2400	1200

In all cases, the maximum measured stresses occurred at the junction between nozzle and cylinder. To examine the maximum stresses, stress ratios were considered. These ratios were determined by dividing the maximum absolute principal stress value at a point by a nominal membrane stress value. The membrane hoop stress in the cylinder was used as the nominal stress level for the pressure loading, and the maximum membrane bending stresses in the nozzle (computed by Mc/I) were used for the moment loadings.

The variations of the experimentally determined maximum stresses around the junction between nozzle and cylinder are shown in Fig. 10 for both models and for each of the three loadings. In each case, the stresses shown were determined from the strain-gage rosettes

*The assumption of zero bending rotation about lines parallel to the nozzle axis is a reasonable one and is equivalent to the assumption, often made in analyzing the local bending in cylindrical shells, that changes in curvature in the hoop direction are negligible compared with those in the axial direction. Bailey and Hicks [6], for example, made the latter assumption in examining the effects of a bending moment applied to the nozzle of a nozzle-to-spherical shell attachment.

immediately adjacent to the junction, and of the four possible maximum stress distributions — cylinder inside and outside and nozzle inside and outside — those shown produced the largest stresses in each case.

The estimated maximum stress ratio at the junction is also shown in Fig. 10 for each case. These estimated maximums were obtained by extrapolating the experimentally determined principal stress distributions along each gage line to the peak stresses at the junction. These estimated maximum stress ratios are summarized below:

	Model 1	Model 3
Internal pressure	13.3	2.6
Out-of-plane moment on nozzle	35.3	5.1
In-plane moment on nozzle	10.0	4.0

In the case of model 1, the maximum stress occurred at 180° (see Fig. 3) for internal pressure, 270° for the out-of-plane moment, and 300° for the in-plane moment. In the case of model 3, the maximum stress occurred at 0° (see Fig. 4) for internal pressure, 270° for the out-of-plane moment, and 0° for the in-plane moment. It should be emphasized that the maximum stress estimates are based on a consideration of the stresses along gage lines only; this does not preclude the existence of slightly higher ratios at locations between gage lines.

The measured and predicted stress distributions along the gage lines at the positions of maximum stresses for the first model are shown in Figs. 11, 12, and 13, respectively. The stresses are shown for the outside and inside surfaces of the cylinder and for the outside and inside surfaces of the nozzle as a function of distance from the junction of nozzle and cylinder midsurfaces. The heavy lines are the predicted stresses while the fine lines through the experimental points show the measured distributions. The solid lines in each case represent the transverse stresses, which are perpendicular to the gage lines, and the dashed lines represent the longitudinal stresses, which are parallel to the gage lines. The solid lines can thus be compared with each other and the dashed lines can be compared with each other.

The agreement between theory and experiment is reasonably good for these three cases except that the stresses at the junction, where the maximums occur, are at times underestimated somewhat by the finite element predictions. The general shape and distribution of the stresses are, however, well predicted by the theory.

The measured and predicted stress distributions along the gage lines at the positions of maximum stresses for model 3 are shown in Figs. 14, 15, and 16, respectively. With the exception of the transverse stress on the inner surface of the nozzle in Fig. 16, the agreement between theory and experiment is again reasonably good, even though the nozzle of the third model was thicker than what is normally assumed for the limit of applicability of thin-shell theory. It should be emphasized that the predictions shown in Figs. 15 and 16 for the moment loadings were obtained with the sixth degree of freedom redefined, as discussed in the previous section.

5. SUMMARY AND CONCLUSIONS

Two idealized cylinder-to-cylinder shell models were tested and the experimentally determined elastic stress distributions were compared with predictions from a typical thin-shell finite element computer program. The first model was very thin, and the nozzle diameter was one-half the cylinder diameter. The second model had a relatively thick, small

diameter nozzle with a diameter-to-thickness ratio that placed it outside the usual bounds for applicability of thin-shell theory.

The maximum stresses in both models occurred at the junction of nozzle and cylinder. For the three loadings considered — internal pressure and out-of-plane and in-plane moments applied to the nozzles — the maximum experimentally determined stress ratios for the first model varied from 10.0 to 35.3, while for the second model they varied from 2.6 to 5.1. Thus the junction stresses were considerably higher in the first model than in the second.

The analytical predictions were obtained from a thin-shell finite element program that used flat-plate elements and which considered five degrees of freedom per node in the final assembled equations. The comparison of these particular finite element predictions with the experimental results showed reasonably good overall agreement. It was found that the neglect of a sixth degree of freedom required some caution in application. Rather than neglecting the component of bending rotation about normals to the nozzle surface of the second model, it was necessary to modify the program so that rotations about lines parallel to the nozzle axis were neglected. The inclusion of a sixth degree of freedom in the equations for the assembled structure would, of course, overcome this difficulty, but the savings in computer time obtained with a five degree of freedom formulation is significant, particularly in those cases where design stress intensity information is to be generated by parametric studies.

In conclusion, the finite element formulation used was chosen simply as a representative analysis, but it does appear to be adequate for most engineering purposes. This is not to say that there is not room for improvement in the analytical predictions; the inclusion of a sixth degree of freedom for flat-plate elements or the use of curved shell elements would be expected to give more accurate predictions.

6. ACKNOWLEDGEMENTS

The analytical and experimental studies reported herein required the assistance and cooperation of many individuals, both within the Oak Ridge National Laboratory and at outside organizations. The authors are thus deeply indebted to these people for their contributions and take this opportunity to express their appreciation.

The finite element computer program used in the analyses was developed at the University of California, Berkeley, and a number of the actual analyses reported in this paper was performed there. The authors wish to acknowledge the help and advice of R. W. Clough of the University of California and of Ojars Greste, a former graduate student at Berkeley. Finally, the assistance of C. P. Johnson, who wrote the original program and who, as an Oak Ridge National Laboratory consultant, suggested the program modifications for the second model, is acknowledged.

REFERENCES

[1] JOHNSON, C. P., The Analysis of Thin Shells by a Finite Element Procedure, Report No. 67-22, Department of Civil Engineering, University of California, Berkeley (September 1967).

[2] JOHNSON, C. P., SMITH, P. G., A Computer Program for the Analysis of Thin Shells, Report No. 69-5, Department of Civil Engineering, University of California, Berkeley (August 1967).

[3] GRESTE, OJARS, Finite Element Analysis of Tubular K Joints, Report No. UCSESM 70-11, University of California, Berkeley (June 1970).

[4] GRESTE, OJARS, A Computer Program for the Analysis of Tubular K Joints, Report No. 69-19, Department of Civil Engineering, University of California, Berkeley (November 1969).

[5] CLOUGH, R. W., TOCHER, J. L., "Finite Element Stiffness Matrices for the Analysis of Plate Bending," Proceedings of Conference on Matrix Methods in Structural Mechanics, Report No. AFFDL-TR-66-80, Wright-Patterson Air Force Base (November 1966).

[6] BAILEY, R., HICKS, R., "Localized Loads Applied to a Spherical Pressure Vessel Through a Cylindrical Insert," J. of Mech. Engineering Science, 2(4), 302 (1960).

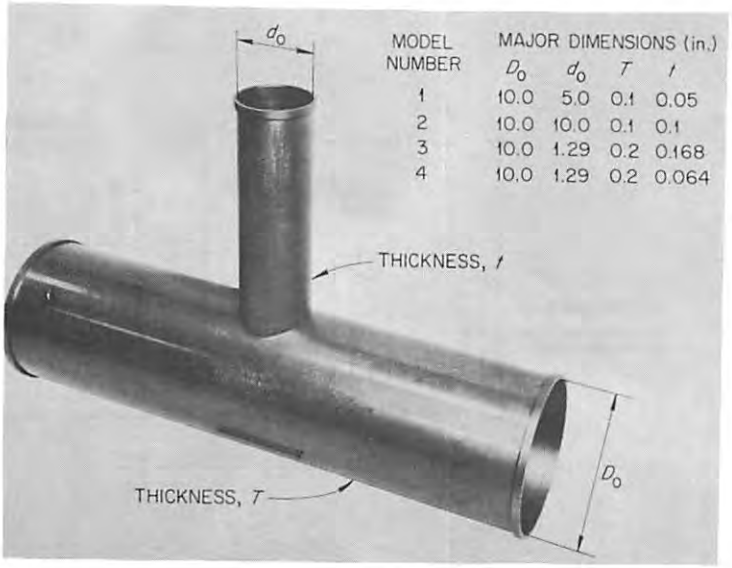

Fig. 1. Cylinder-to-Cylinder Shell Model 1 and Table Showing Dimensions of Four Models in Test Series.

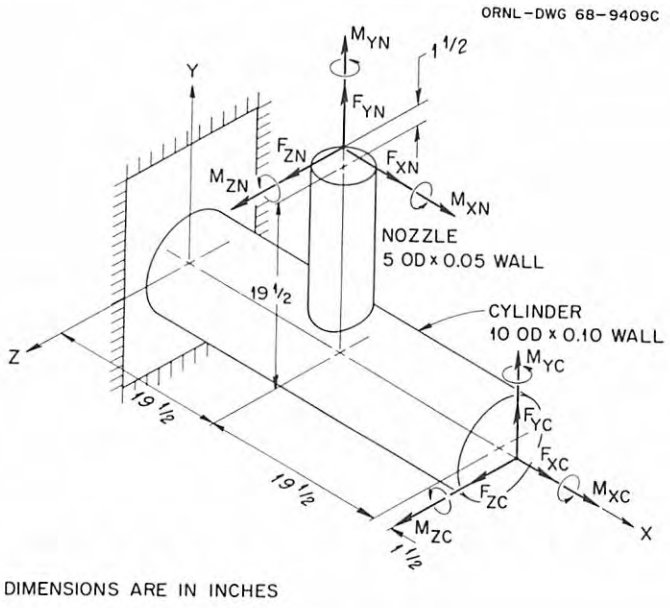

Fig. 2. Schematic of First Model Showing Applied External Loadings.

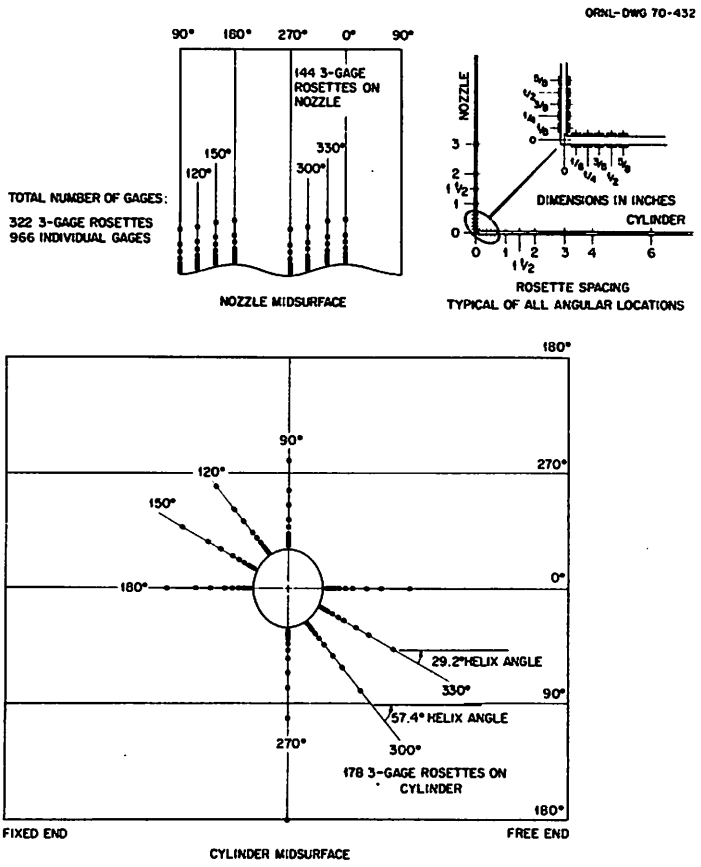

Fig. 3. Strain-Gage Layout for Model 1.

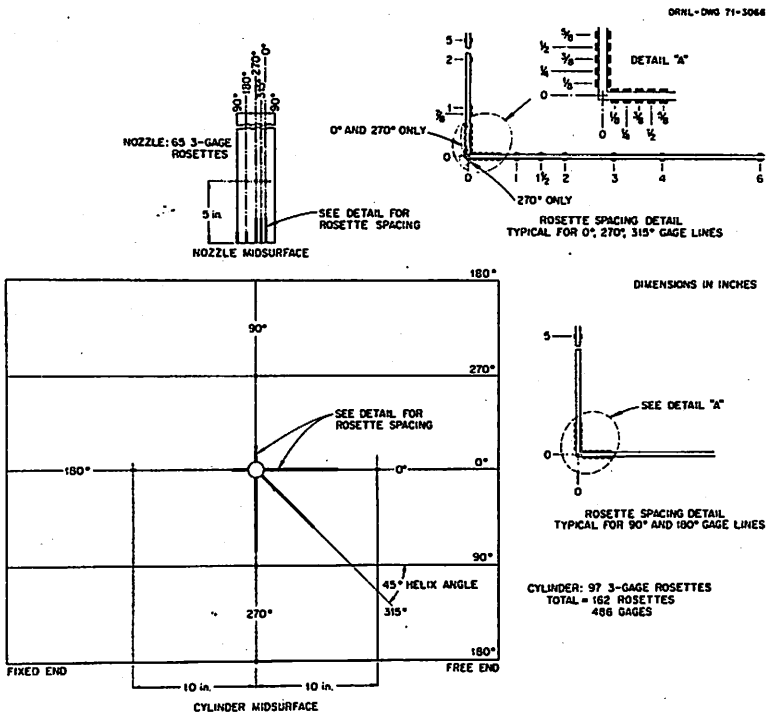

Fig. 4. Strain-Gage Layout for Model 3.

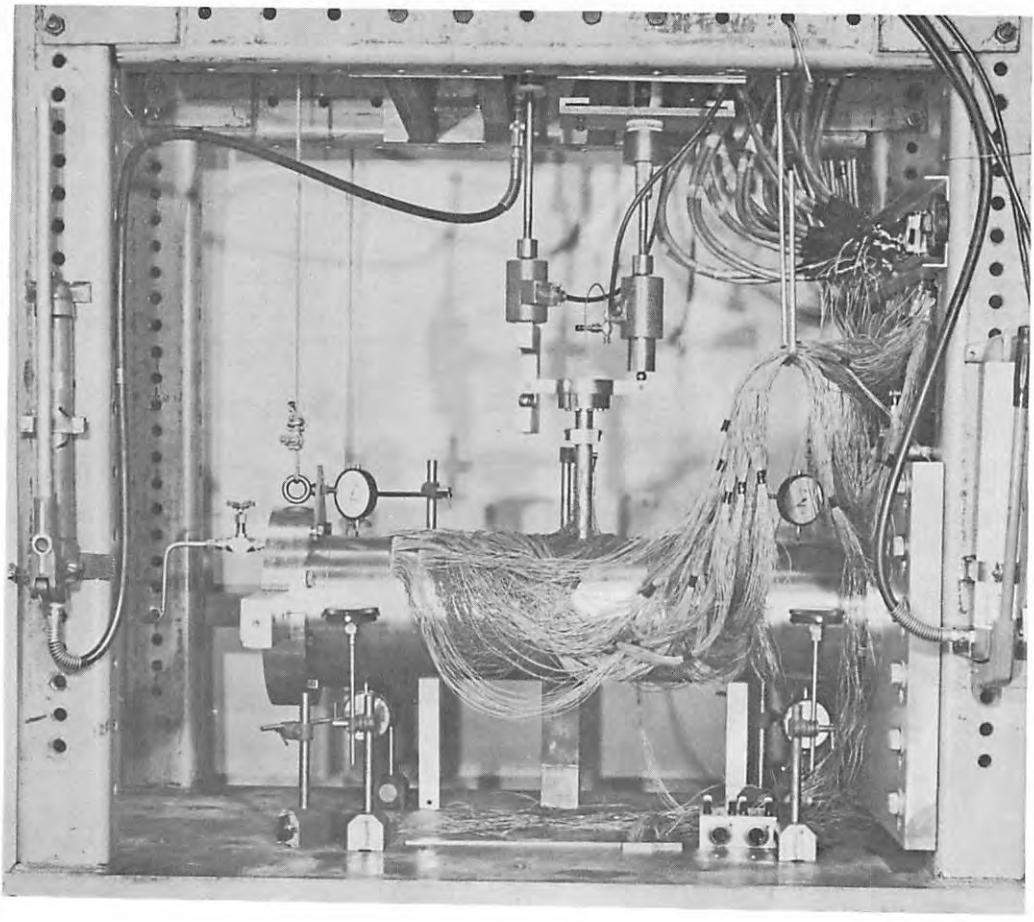

Fig. 5. Model 3 in Test Frame Being Subjected to an In-Plane Moment Loading on the Nozzle.

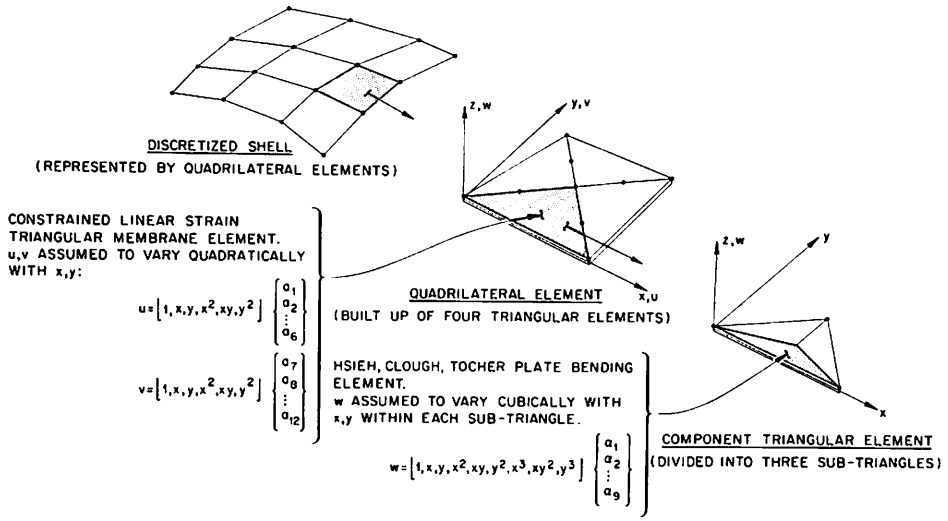

Fig. 6. Quadrilateral Element and Component Triangles.

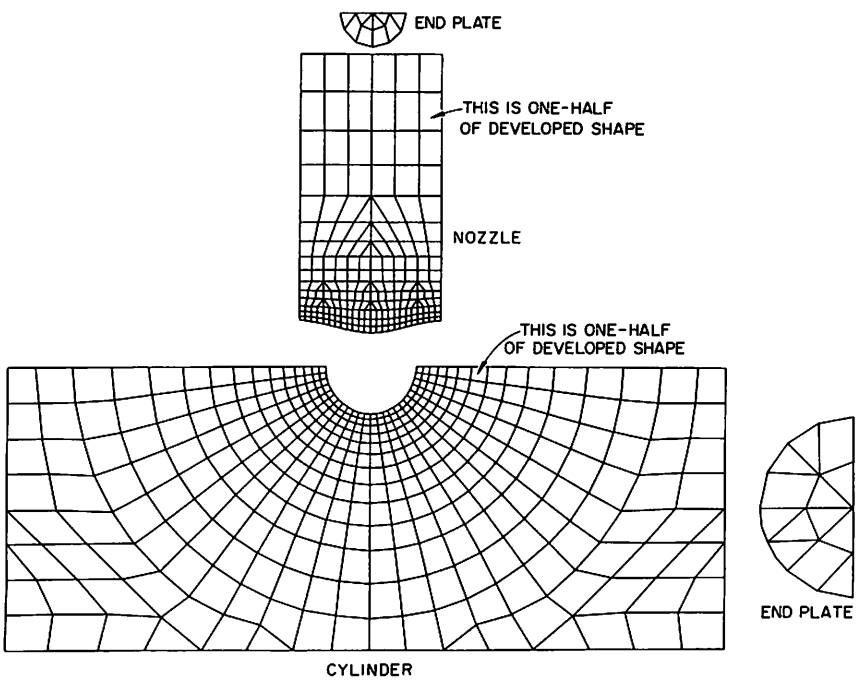

Fig. 7. Finite Element Idealization of Model 1.

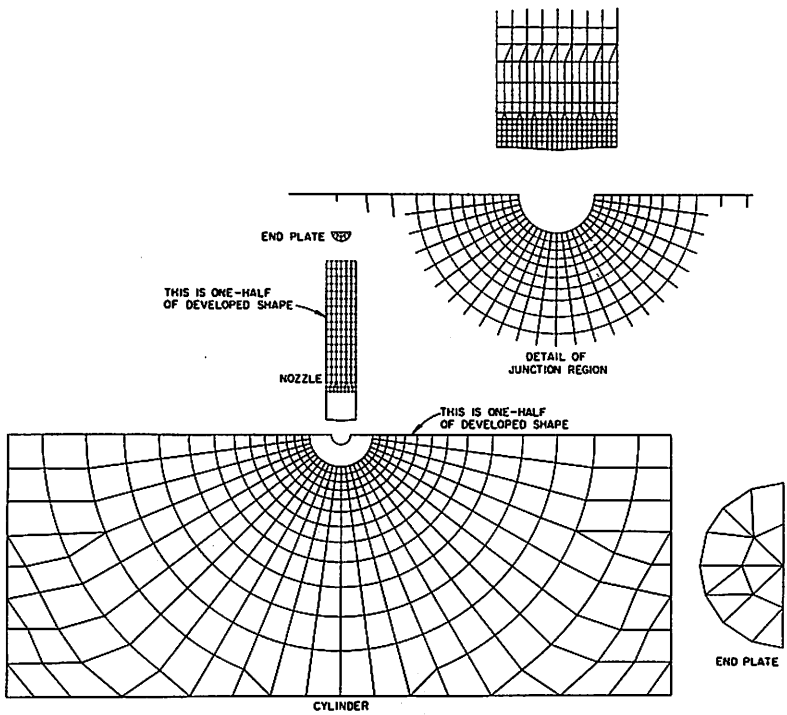

Fig. 8. Finite Element Idealization of Model 3.

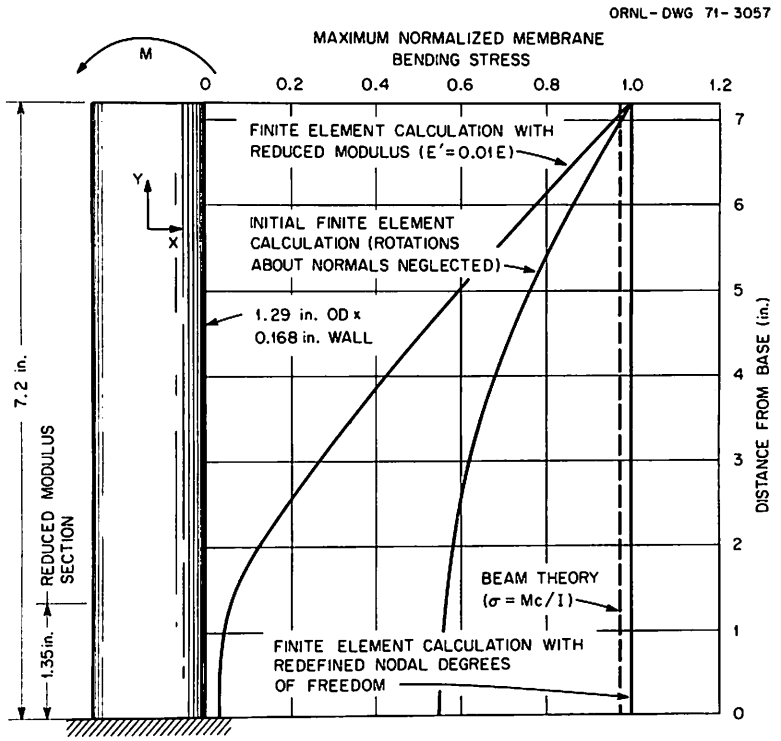

Fig. 9. Example Problem Demonstrating Effects of Neglecting Component of Bending Rotation About Normals to the Surface of Slender Nozzle.

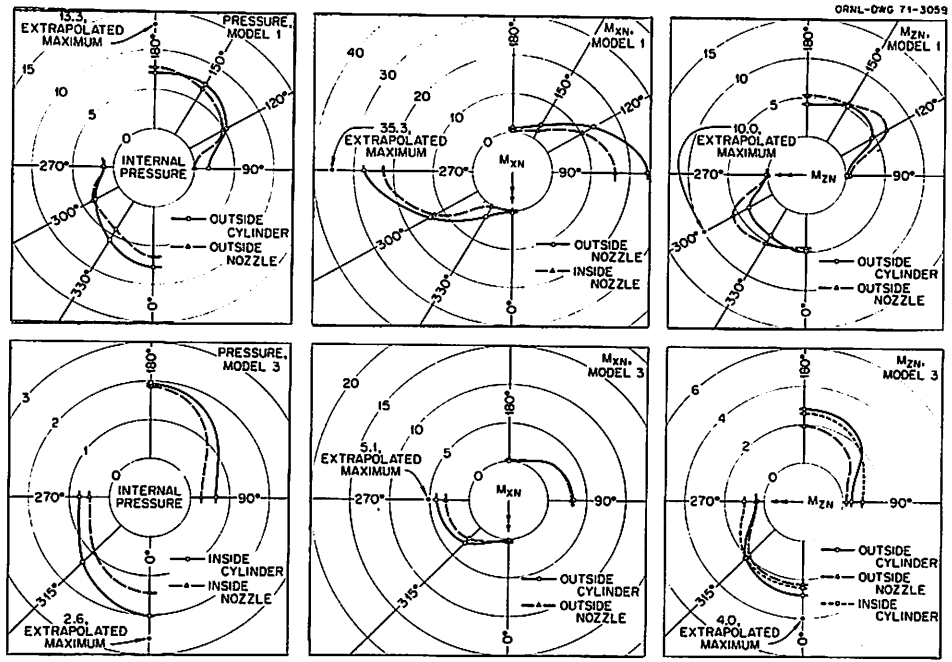

Fig. 10. Variations of Maximum Principal Stress Ratios Around Nozzle-Cylinder Junction. Note that the plotted quantities are absolute values.

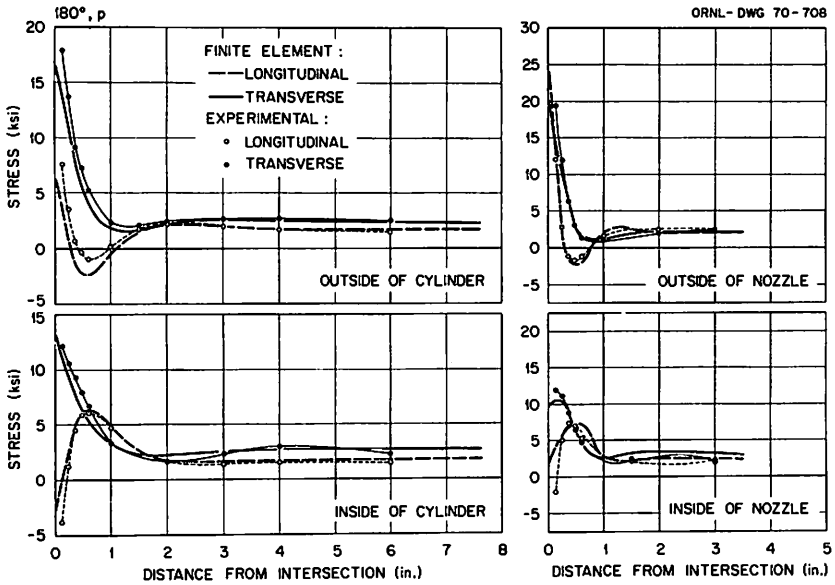

Fig. 11. Measured and Predicted Stress Distributions at 180° in Model 1 for Internal Pressure of 50 psi.

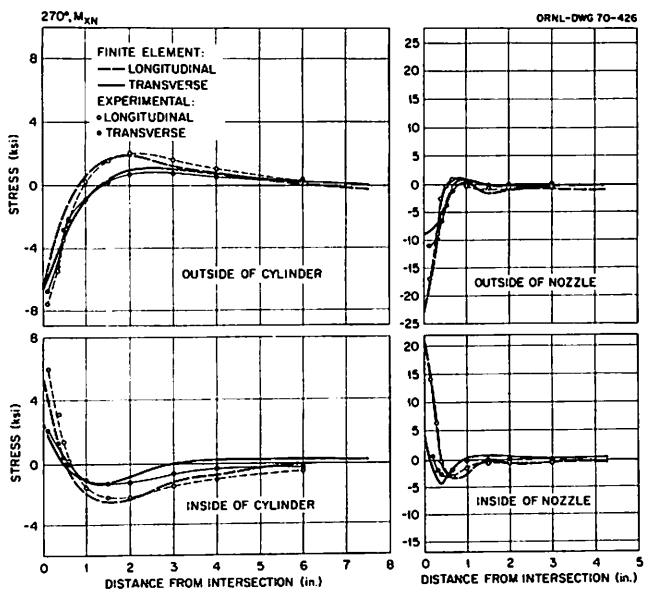

Fig. 12. Measured and Predicted Stress Distributions at 270° in Model 1 for an Out-of-Plane Moment of 600 in.-lb on Nozzle.

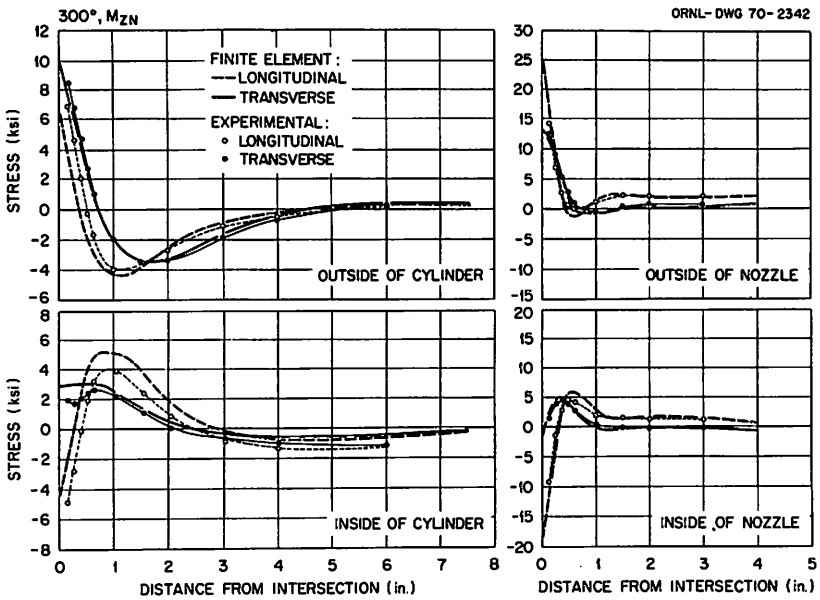

Fig. 13. Measured and Predicted Stress Distributions at 300° in Model 1 for an In-Plane Moment of 2400 in.-lb on Nozzle.

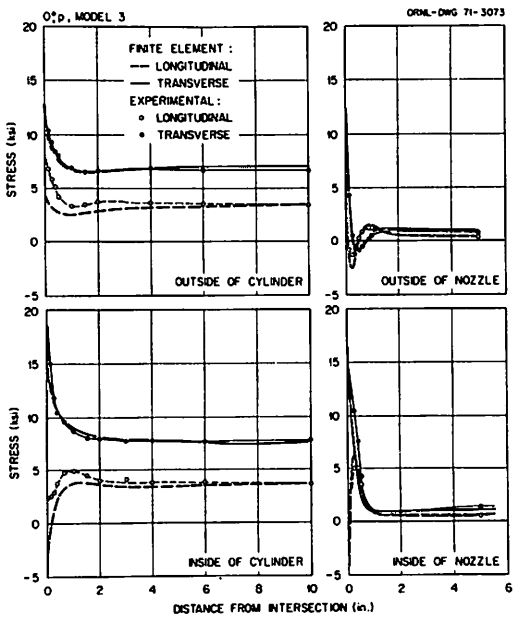

Fig. 14. Measured and Predicted Stress Distributions at 0° in Model 3 for Internal Pressure of 300 psi.

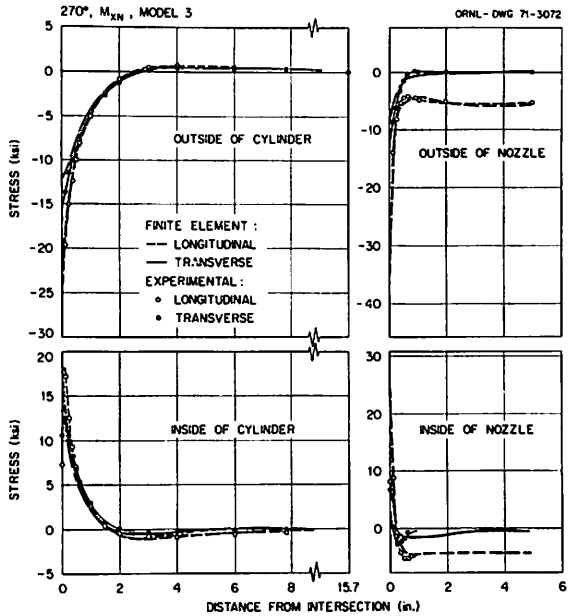

Fig. 15. Measured and Predicted Stress Distributions at 270° in Model 3 for an Out-of-Plane Moment of 800 in.-lb on Nozzle.

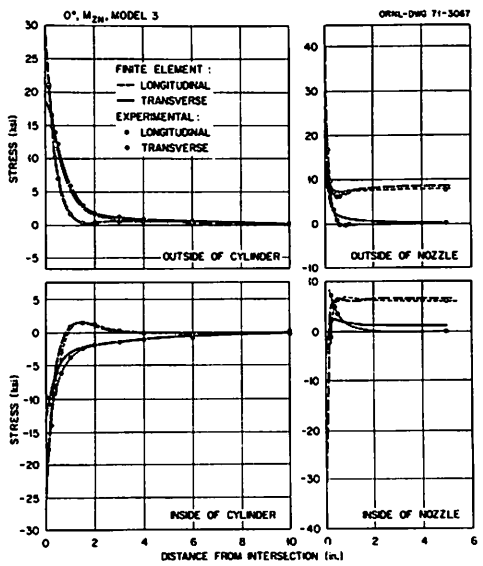

Fig. 16. Measured and Predicted Stress Distributions at 0° in Model 3 for an In-Plane Moment of 1200 in.-lb on Nozzle.

DISCUSSION

Q D. H. VAN CAMPEN, The Netherlands

There have been presented during this session two finite (thin shell) element approaches for the cylinder-to-cylinder intersection problem at equal or nearly equal cylinder diameters. Is it possible for designer's convenience to indicate which one gives the most reliable results ?

A W. L. GREENSTREET, U. S. A.

With the information at hand, it is prudent for me only to repeat that the finite element method used in our analyses gives reasonably good overall agreement with the experimental results that we obtained. Thus, it appears to be adequate for engineering purposes. The designer's choice should depend on the particular needs of the application.

A E. GIENCKE, Germany

The methods, used by Greenstreet and Ando, cannot be compared directly because Greenstreet has used the deformations method with plane plate elements and Prof. Ando a mixed method for curved shell elements.